STUDY ON PARAMETER VARIATION OF AN INDUSTRIAL COMPUTED TOMOGRAPHY SIMULATION TOOL CONCERNING DIMENSIONAL MEASUREMENT DEVIATIONS

Michael REITER[a], Christoph HEINZL[a], Dietmar SALABERGER[a], Daniel WEISS[b], Johann KASTNER[a]

[a]*Upper Austria University of Applied Sciences, Wels Campus, Austria*
[b]*Carl Zeiss Industrial Metrology, Oberkochen, Germany*

Abstract. This paper presents a simulation aided study on measurement parameters for industrial X-ray computed tomography (CT). The used simulation tool is able to predict the results of real CT measurements and could help technicians in measurement technology to minimize artifacts by determining applicable measurement parameters. We present a procedure to determine utilizable measurement parameters for CT, apply this procedure and generate 22 different parameter combinations for a selected test part. For all these parameter combinations CT measurements and simulations are done, to further investigate their influence on a metrology task. We use Carl Zeiss Calypso® to characterize measurement features of the selected test part. Finally a comparison of the gained feature properties is done, using dimensional measurements of a tactile coordinate measuring machine (CMM) as a reference for CT measurements and nominal values of the initial CAD model for simulated CT results.

1 Introduction and Motivation

X-ray computed tomography is a common method for non-destructive testing. A relatively new and challenging application in the field of computed-tomography (CT) is metrology, which has to fulfill the demands of today's standards for quality control. The achievable measurement deviations mainly depend on the quality of CT data, on the knowledge of the exact system geometry and in addition on the used evaluation algorithms. The quality of CT data is influenced by the used CT device parameters like X-ray source voltage, anode current, filter plates, detector integration time, number of projections, position and orientation of the specimen in the X-ray cone and the measurement conditions. Either the resulting data includes sharp edges and few artifacts or a subsequent evaluation procedure will cause elevated measurement deviations. Selection and optimization of these parameters nowadays is done by an experienced system operator, which leads to subjective measurement results. A CT simulation software is able to do this optimization process automatically and generates user independent device parameters by additionally saving preparation time.

Monte-Carlo simulations [1] would be able to represent the interactions of X-rays with matter very accurately, but due to their high computational cost, Monte-Carlo simulations are not suitable for the required optimization of a complete CT scan with a high number of projections. Therefore a time optimized simulation for industrial cone beam CTs, which models all essential effects at sufficient accuracy is used for the mentioned variation and optimization of measurement parameters.

Criteria for the optimization could be selected for non-destructive testing or metrology. This paper focuses on metrology by evaluations of measurement features with a common tool for metrology – Carl Zeiss Calypso® [2][3].

2 Modeling of a polychromatic X-ray cone beam computed tomography system

A cone beam computed tomography (CBCT) system as shown in Figure 1 consists of an X-ray source, a rotary table and an X-ray sensitive detector. During a full incremental turn of the specimen, penetration images which contain the spatial X-ray attenuation are recorded. Using these images it is possible to reconstruct the complete inner and outer structure of the specimen. The reconstruction method used within this work is the FDK filtered back-projection algorithm published by Feldkamp et al. [4].

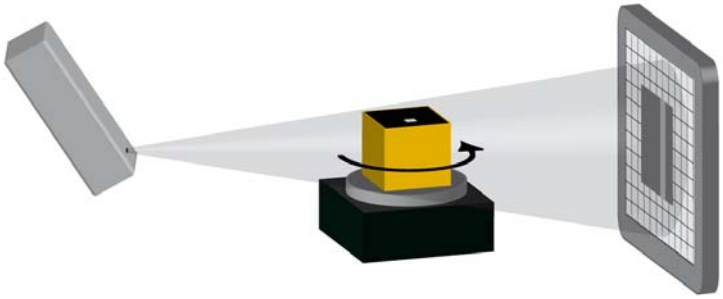

Figure 1: Schematic of a cone beam computed-tomography system

The modeling process of a CBCT system has to cover the following sections, an X-ray source model, interactions of X-rays with the object matter and the development of a detector model.
The simulation uses an X-ray source model published by H. Ebel [5]. This model allows the calculation of polychromatic spectra consisting of Bremsstrahlung and characteristic radiation. Real X-ray sources have a finite focal spot size, which causes geometric blur and is modeled by a convolution operation [6].
The virtual specimen is represented by a model consisting of a triangle surface mesh and an assigned material, which may be defined by mass-weighted molecular formulas. The elemental cross sections and differential cross sections are given by Brunneti et al. [7]. A ray-tracing algorithm [8] calculates the attenuation lengths d along an ideal ray from the source to a point on the detector, where the whole sensor area has to be covered with ideal rays. Subsequently the X-ray source spectrum is attenuated by the determined attenuation lengths, weighted with a detector efficiency and finally summed up to grey values. Effects caused by beam hardening are thus completely covered.
In addition the simulation tool offers the opportunity to consider noise and first order scatter effects within the inspected specimen. With some approximations it is possible to reduce the scatter process to N_E convolutions, where the convolution kernel has twice the size of the detector dimension and N_E is the number of used energy channels. Furthermore detector inherent scatter is modeled by convolutions with large point spread function (PSF) kernels.
The whole CT simulation process has been implemented on the CPU using C++ and on the GPU additionally using the NVidia toolkit CUDA [9].

3 Investigation and results

The major goal of the investigation is to determine reliable and robust CT parameter sets for a specific metrology task defined in chapter 3.3 on a selected specimen described in chapter 3.1.
Usually the selection and optimization of parameters is done by the system operator, which leads to subjective measurement results. The achieved image quality depends on the experience of the system operator and is not reproducible. The definition of some selection criteria with some appropriate thresholds would lead to a user independent image quality. Such criteria can be acquired and calculated by

preliminary measurements or by simulations. The following paragraphs describe a suggestion for a parameter selection procedure based on a simulation tool for computed tomography.

3.1 Definition of a specimen

The specimen tp07 shown in Figure 2a, is a step cylinder made of aluminum EN AW-7075 (Figure 2b). Tp07 consist of 5 steps, each 10 mm in height, the outer diameter is increasing from 15 mm to 55 mm in steps of 10 mm. The central drill hole has a diameter of 8 mm. Similar step cylinders are used by the VDI/VDE technical committee 3.33 to develop the guideline VDI/VDE 2630 for „Computed tomography in industrial metrology“.

(a)

EN AW-7075		
element	**mass weight**	**density**
Al	88,42 %	2,8 g/cm³
Si	0,4 %	
Fe	0,5 %	
Cu	1,6 %	
Mn	0,3 %	
Mg	2,5 %	
Cr	0,23 %	
Zn	5,6 %	
Ti	0,2%	
Zr	0,25 %	

(b)

Figure 2: Shows the selected test part tp07 defined by a surface mesh consisting of 400.000 triangles (a) and the specification of the aluminum alloy EN AW-7075 (b)

3.2 Determination of utilizable measurement parameters for a CT measurement

The first step is to define a circular source-detector trajectory for the measurement of the specimen. Figure 3 shows four different orientations of test part 07 in the cone beam. There is a significant change in the appearance and strength of FDK artifacts in the reconstructed data. These artifacts are caused by lacking information of the specimen in the acquired radon space data, when using a cone beam and a circular trajectory [10]. A reduction of these artifacts could be achieved by avoiding planes perpendicular or almost perpendicular to the rotation axis. In Figure 3a the alignment with the shortest possible maximum penetration length d_{max} but with most of the FDK artifacts is shown, these artifacts appear at surface planes perpendicular to the rotation axis. Rotating the test part around x results in a reduction of these artifacts, changes d_{max} and increases the possible voxel size of reconstructed data. A rotation by 10° is a good compromise between this three criteria for a cone angle of 14.89°, therefore it is selected for the acquisition (Figure 3c).

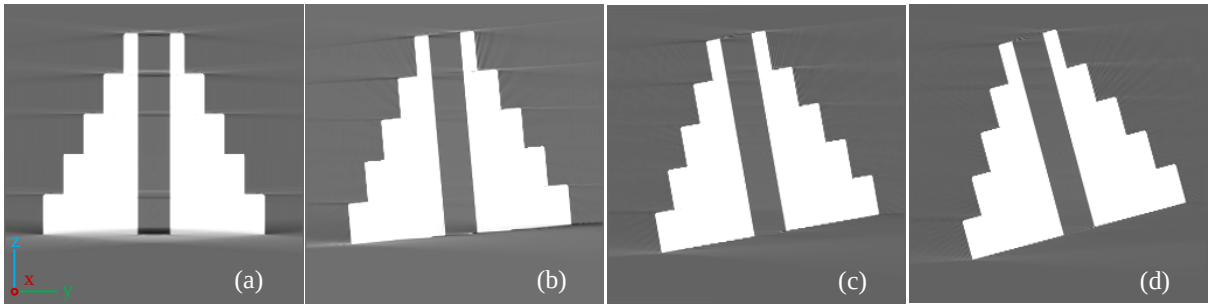

Figure 3: Shows reconstructed data with different orientations of test part 07 in a cone beam with monochromatic X-rays, the rotation around the x-axis is varied, (a) 0° with d_{max} = 54.565 mm, (b) 5° with d_{max} = 55.087 mm, (c) 10° with d_{max} = 55.208 mm and (d) 15° with d_{max} = 55.112 mm; tested at a voxel size of 72.794 µm and a cone angle of 14.89°

The maximal possible magnification for the selected alignment results in a voxel size of 68.11 µm and a maximum penetration length d_{max} of 54.553 mm. Now it is possible to compute expected X-ray intensities respectively gray values after the attenuation by material with penetration lengths d in the range $d=0…d_{max}$. This calculation is possible via the Lambert-Beer law [9], if the material composition is known, a model for the calculation of X-ray source spectra and the detector efficiency is available. The spectrum of a direct beam source is changeable and mainly defined by the parameters acceleration voltage, prefilter material and thickness, if the target material is considered as constant.
In detail the calculation of gray values is done by applying the Lambert-Beer law according to Equation 1 for a selected number of energy channels. Afterwards the photons emitted by the source are weighted with the detector efficiency DE(E) in the energy channels E and summed up to a gray value gv(d) (Equation 2). $P_0(E)$ and P(E) are the number of X-ray photons before and after the linear attenuation process in the energy channel E. Furthermore μ_{mat} is the mass weighted sum of elemental linear X-ray attenuation coefficients µ as given by Brunneti et al.[7]. For the comparison of a real measured gray value and simulated gray value one has to consider the gray value caused by the dark current of the detectors photo diode, which shows a dependency on the integration time T (Equation 3).

$$P(E,d) = P_0(E).e^{-\mu_{mat}(E).d} \tag{1}$$

$$gv(d) = \sum_{E=0}^{E_{max}} P(E,d).DE(E) \tag{2}$$

$$gv_{real\,detector}(d,T) = gv(d) + gv_{dark\,current}(T) \tag{3}$$

Computation of Equation 1 and 2 for d=0 gives the maximum appearing gray value gv(d=0) in the projection image stack. The calculation for $d=d_{max}$ gives the lowest gray value $gv(d=d_{max})$.
A combination of acceleration voltage U and prefilter plate defines $P_0(E)$ and is suitable for measurements if the resulting contrast of the projection images according to Equation 4 is within a detectable range bounded by $contrast_{min}$ and $contrast_{max}$ (Equation 5). $Contrast_{min}$ is the border for the lowest attenuation and $contrast_{max}$ the highest attenuation not anymore detectable. These borders avoid noisy signals, at the upper or lower limits of the detectors dynamic range, to exceed the acquirable range.

$$contrast = 1 - \frac{gv(d = d_{max})}{gv(d = 0)} \tag{4}$$

$$contrast_{min} < contrast < contrast_{max} \tag{5}$$

The maximal gray value gv(d=0) should be maximized for every combination U and prefilter by adjusting the X-ray tube's anode current I and integration time to maximize the signal to noise ratio. A boundary condition is that the blur caused by the focal spot is negligible. Additionally the X-ray tubes minimum and maximum current as well as power have to be considered. Checking all these conditions should first be done for the shortest possible integration time T of the detector. If one of the boundary conditions could not be fulfilled the integration time has to be increased until they are or the combination U and prefilter is not suitable. Increasing the integration time will increase the measurement time of the CT scan which is mainly determined by the number of projections, the detectors integration time and averaging, the number of skipped images to avoid effects caused by image lag and the manipulation time of the rotary table.

Figure 4 points out that scatter is not negligible for the presented specimen. Nevertheless the preselection of suitable parameters should be done considering only the ideal attenuation of X-rays, because if gv(d=d_{max}) is 0 the projection image does not contain the full projection information of the specimen and scattered photons will just lift the intensities above 0 without delivering object information. The reconstruction of such images results in blurred structures, where the back-projections contain incom

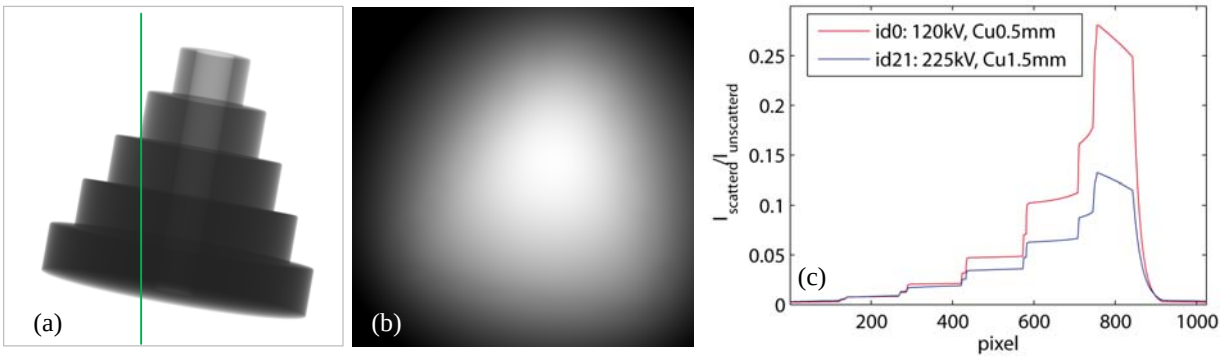

Figure 4: Simulated projection image of parameter set id0 (a) unscattered intensity and (b) scattered intensity with a maximum ratio $I_{scatterd}/I_{unscattered}$ of 0.28. (c) shows a plot of the id0 and id21 ratio along the green line in (a), the parameter set id21 shows its maximum $I_{scatter}/I_{unscattered}$=0.13 also along the green line

id	U	I	T	prefilter thickness	measure-menttime	contrast	gv(d=0)	gv(d=d_{dmax})	attenuation linearity
	[kV]	[A]	[s]	[mm]	[min]				
0	120	522	2	0.5	59.46	0.9875	58053	722	0.850
1	135	448	0.5	0	36.96	0.9938	58050	358	0.574
2	135	379	2	0.5	59.46	0.9840	58053	922	0.849
3	150	371	0.5	0	36.96	0.9922	58050	447	0.578
4	150	291	2	0,5	59.46	0.9811	58053	1092	0.849
5	165	313	0.5	0	36.96	0.9909	58050	524	0.581
6	165	233	2	0.5	59.46	0.9787	58053	1231	0.848
7	165	385	2	1	59.46	0.9719	58053	1628	0.902
8	180	269	0.5	0	36.96	0.9898	58050	589	0.585
9	180	192	2	0.5	59.46	0.9768	58053	1344	0.848
10	180	312	2	1	59.46	0.9695	58053	1767	0.901
11	195	235	0,5	0	36.96	0.9888	58050	644	0.589
12	195	324	1	0.5	44.46	0.9753	58051	1433	0.847
13	195	260	2	1	59.46	0.9676	58053	1878	0.900
14	210	206	0.5	0	36.96	0.9880	58050	691	0.593
15	210	278	1	0.5	44.46	0.9740	58051	1506	0.847
16	210	221	2	1	59.46	0.9660	58053	1968	0.900
17	210	316	2	1.5	59.46	0.9597	58053	2337	0.925
18	225	183	0.5	0	36.96	0.9873	58050	732	0.599
19	225	241	1	0.5	44.46	0.9730	58051	1564	0.847
20	225	190	2	1	59.46	0.9648	58053	2041	0.898
21	225	271	2	1.5	59.46	0.95829	58053	2421	0.923
22	ideal simulation with monochromatic radiation 100keV								1

Table 1: Shows suitable parameter for a measurement of test part 07 on the described CT system. Detector averaging=1; distance source-object=262mm, 16Bit gray value range, distance source-detector=1538.58mm; voxel size=68.11µm; prefilter plate material copper, no postfilter plate, object rotation around x=10° and z-offset=-23.8mm, source and detector type see chapter 2; d_{max}=55,553mm during a full CT scan

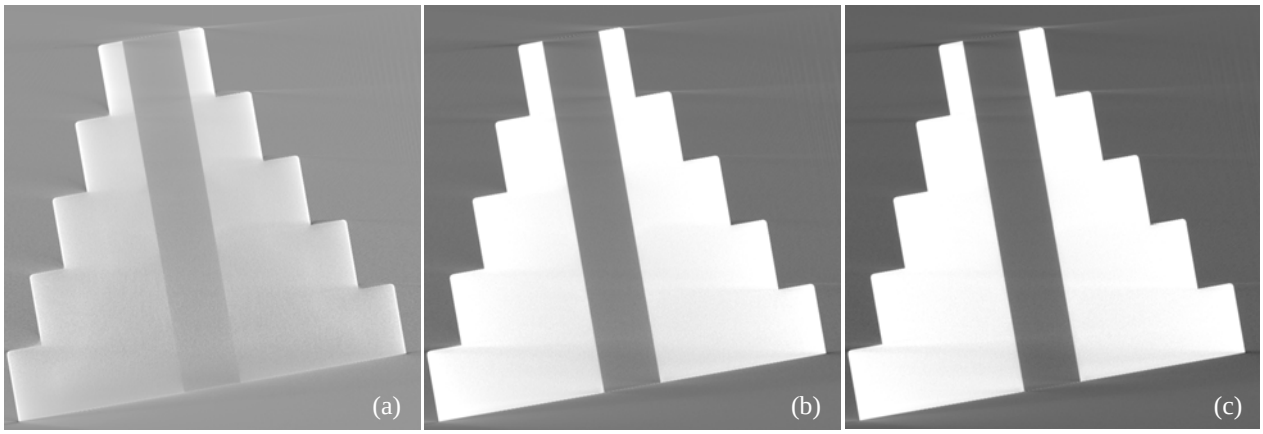

Figure 5: Slice (a) depict artifacts caused by an acceleration voltage of 60kV without a prefilter, where the attenuation is too high at the highest penetration lengths; Examples for utilizable parameters are (b) 120kV data id0 and (c) 225kV data id21, see Table 1 for a listing of the parameters

plete information like shown in Figure 5a.
Table 1 depicts suitable parameter combinations which fulfill all boundary conditions for a measurement of test part 07 on the CT system described in chapter 3.3. The boundary conditions have been checked for all combinations of acceleration voltages from 30 to 225k V in 15 kV steps and copper prefilters with a thickness increasing from 0 to 1.5 mm in steps of 0.5 mm. The calculated value for the minimal possible acceleration voltage is about 120kV. Using less would result in a minimum gray value of 0 at high penetration lengths. Figure 5b and c shows reconstructed slices of the suitable parameters id0 and id21, where id21 seems to be the best parameter combination by visual impression. In addition Figure 6a shows graphs to visualize the beam hardening effect of some parameter combinations by plotting the attenuation(d) according to Equation 5.
Equation 6 is a measure for the attenuation linearity of a parameter combination giving values between 0 and 1. It contains the root mean square error RMSE between a scaled attenuation and an ideal linear attenuation. This ideal linear attenuation is the imaginary line from the origin to the first data point of the attenuation(d) to investigate (Figure 6b). Table 1 contains calculations of this attenuation linearity and depicts that the prefilter thickness is responsible for the curvature of the attenuation and the acceleration voltage has almost no effect. The linearity of attenuation increases from values around 0.57 without a prefilter to 0.92 with a 1.5 mm thick copper prefilter plate. A strong non-linearity of the attenuation (beam hardening) will cause strong cupping artifacts in reconstructed data.

$$\text{attenuation}(d) = \mu.d = \log\left(\frac{gv(d)}{gv(d = 0\text{mm})}\right) \tag{5}$$

$$\text{attenuation linearity} = 1 - \text{RMSE} = 1 - \frac{\sqrt{\sum_{d=0}^{d_{max}} \left(gv_{linear}(d) - gv(d)\right)^2}}{gv(d = d_{max})} \tag{6}$$

3.3 Use of the determined CT parameter combinations for metrology

For all parameter combinations shown in Table 1 X-ray cone beam CT measurements and simulations are done with 900 projections. This results in 22 measurements and 22 simulations, where all effects described in chapter 2 are enabled, plus an idealized artifact free simulation with a monochromatic beam. CT measurements are done on a RayScan Technologies - RayScan 250E device consisting of a Viscom 225 kV-microfocus tube with a tungsten target and a flat panel detector Perkin Elmer RID1640

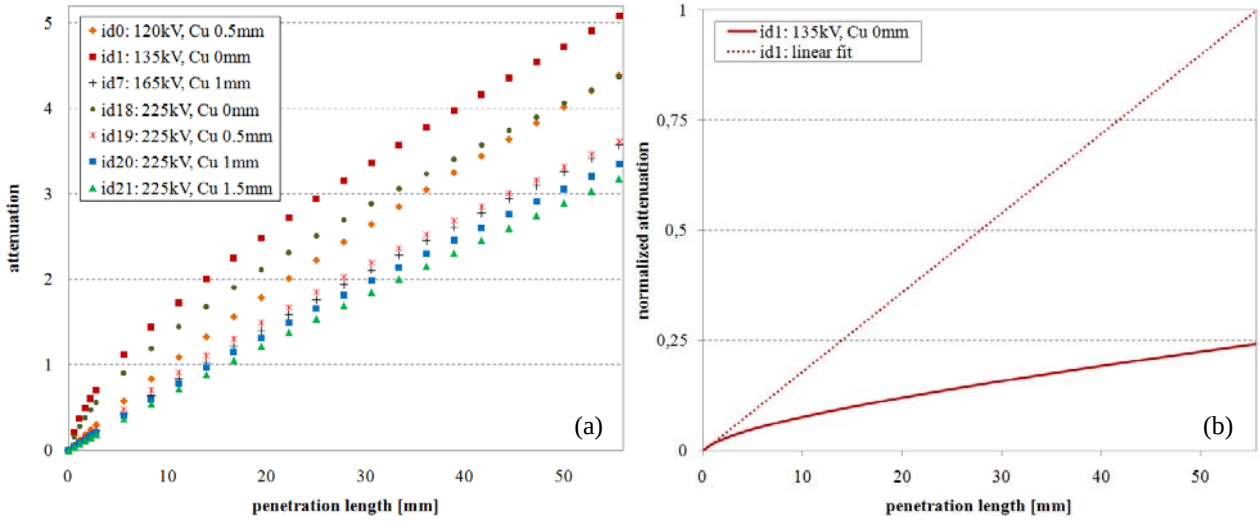

Figure 6: The graphs (a) visualize the beam hardening effect of different parameter sets specified in Table 1, (b) shows an imaginary line from the origin to the first data point of id1, both are normalized to 1

(Image resolution 1024x1024 pixel, pixel size 400µm). Every dataset is evaluated using a common tool for metrology capable to analyze data of coordinate measuring machines (CMMs) and CTs - Carl Zeiss Calypso® Version 4.8.0.6.

The Calypso® inspection plan contains 10 cylinders, 5 are fitted to the outer diameters of the step cylinder and 5 are fitted to the inner drill hole. A cylinder fit is done by fitting three circles at 2.5 mm, 5 mm and 7.5mm height of a step each 10 mm high as shown in Figure 7a. This is done for the outer cylindrical surface and also for the inner drill hole at the same heights. Along the circumference of the circles every 100 µm a surface point is determined, for the biggest diameter of 55 mm this results in 1728 points per circle. The numeration of the steps starts with 1 for the greatest radius at the bottom and ends with 5 at the top step. Reference measurements are done with a CMM using the same inspection strategy.

Before evaluating the 22 real CT measurements the phantom in Figure 7b is used to check and correct geometrical inaccuracies of the CT device used for this investigation.

The graphs of Figure 8 show the evaluation of the outer radii of the cylindrical steps for all parameter

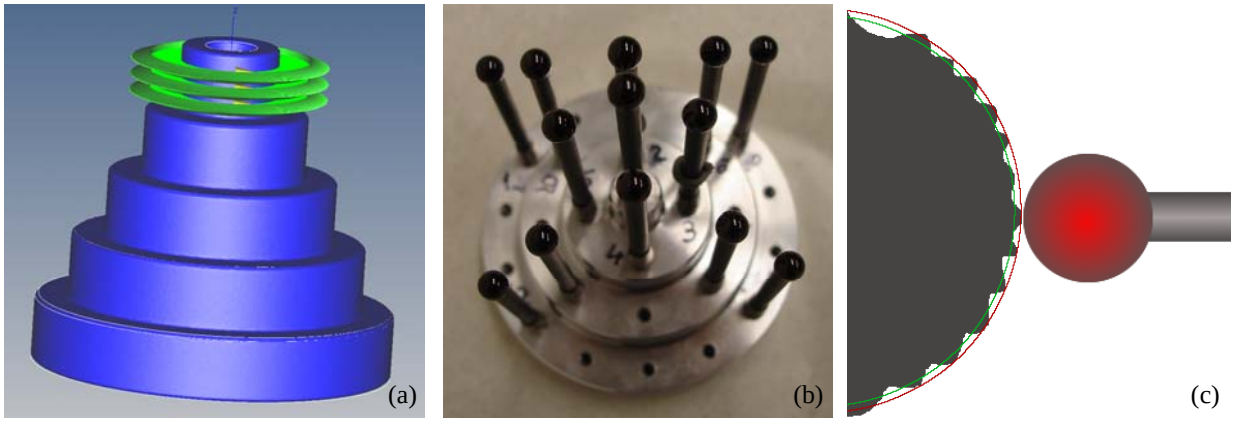

Figure 7: Picture (a) shows the acquisition points for fitting a cylinder to the top step (step 5) and a photo of the phantom (b) used to check and correct the geometry of the CT device, (c) overdrawn systematic deviation between CMM and CT, outer diameter determined with a CMM and the inner with a CT

combinations. Simulations on the left and real measurements on the right depict that the measured radius is reducing with an increasing prefilter thickness. Cause for this is the cupping effect which induces a modification of gray values and affects the edge finding, especially at the outer transition material-air of the specimen. The simulated results also depict a small reduction of deviations by increasing the acceleration voltage. For comparison Figure 8a contains a simulation done with a monochromatic beam of 100keV without scatter, noise and geometric blur (dashed line). Since there is no inaccuracy of the virtual CT all radius deviations are caused by different measurement parameter and their effects. There is a negative offset visible in Figure 8b (measurement) compared to Figure 8a (simulation). One cause

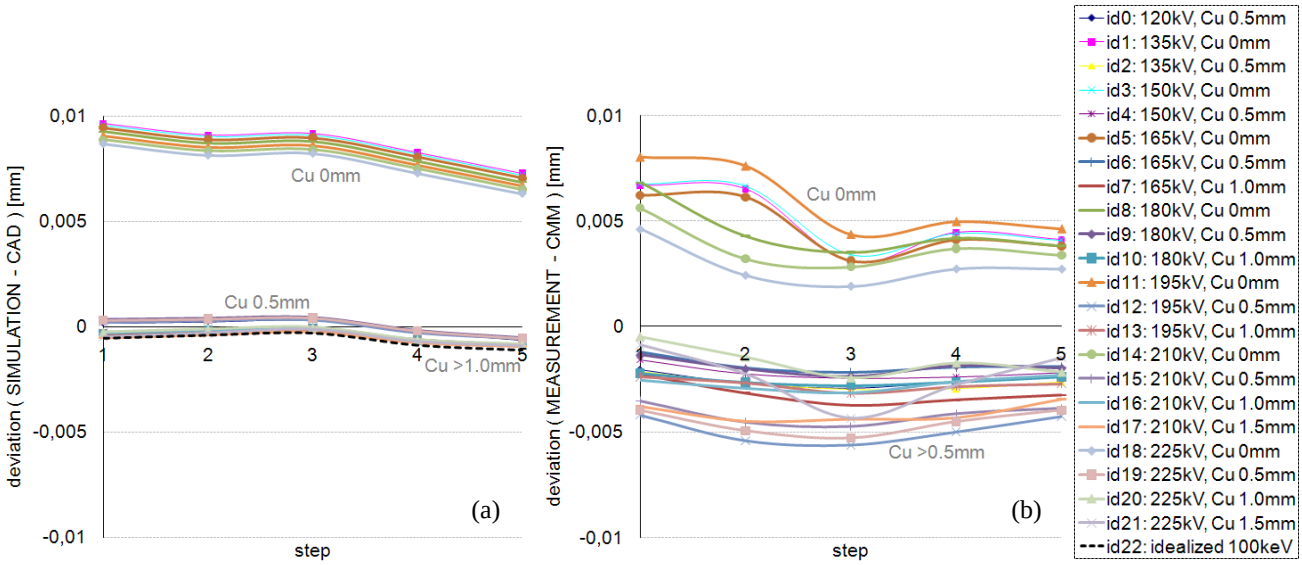

Figure 8: Calypso® evaluation of the outer radii of test part 07, voxel size = 0,06811mm. (a) Simulated results, on the y-axes the radius deviation between CAD and simulated CT, (b) Measurement results, on the y-axes the radius deviation between CMM as a reference and a CT measurement. The x-axes correspond to the different cylindrical steps and radii. Lines connecting data points are drawn to simplify the finding of trends.

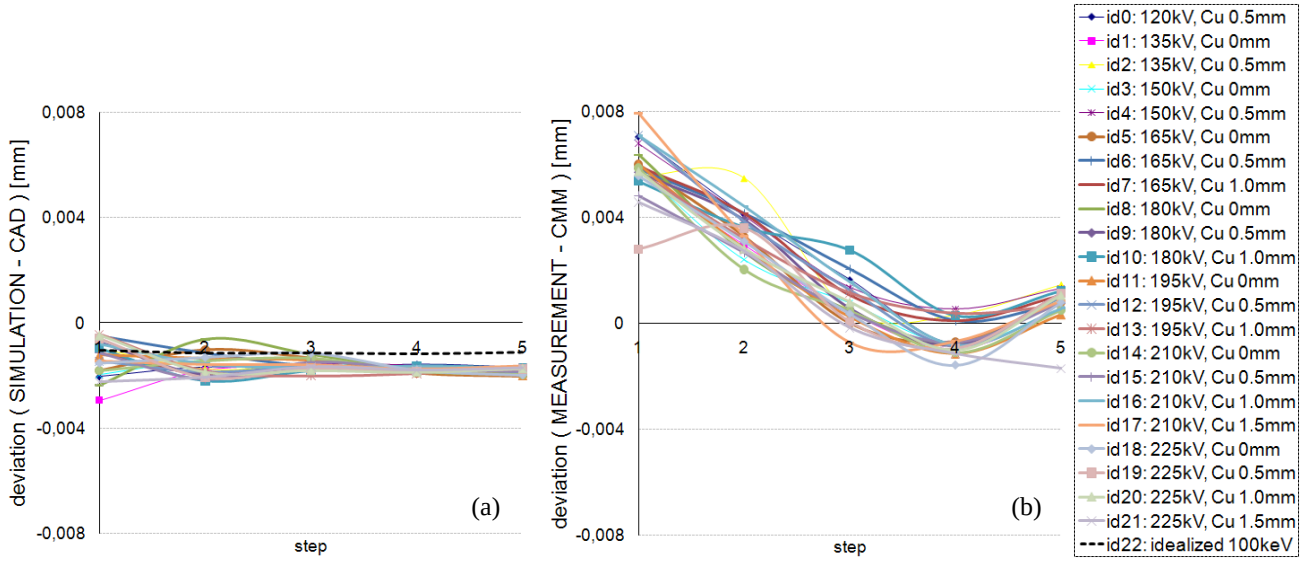

Figure 9: Calypso® evaluation of the inner drill hole radii of test part 07, voxel size = 0,06811mm. (a) Simulated results, on the y-axes the radius deviation between CAD and simulated CT, (b) Measurement results, on the y-axes the radius deviation between CMM as a reference and a CT measurement. The x-axes correspond to the different cylindrical steps. Lines connecting data points are drawn to simplify the finding of trends.

for this offset could be differences between real and simulated edge shapes. Additionally a systematic deviation occurs, caused by the roughness of the real test part, because tactile CMMs consider the roughness of a surface in a different way than CT, due to the finite touching probe size (see Figure 7c). This systematic deviation usually leads to a negative offset between CMM and CT. For the specimen tp07 it should be smaller than the noticed offset of about -3µm visible in Figure 8b. The voxel size of the CT data set seems to be as far as possible correct, because otherwise the deviations in Figure 8b would strongly increase with the measured radius.
In Figure 9 plots of the drill hole radius deviations between CT simulations alternatively measurements and the reference method are shown. There is no systematic change of the drill hole radius caused by different parameters. Real CT measurements show a slight increase of deviations at increased penetration length. These deviations between measurement and simulation are reducing from 1/7 to about 1/35 of the voxel size.
A big benefit of the simulation tool is that a clear separation of effects is possible which makes the selection of parameters easier than using real measurements. The evaluation of the outer radii has shown that beam hardening artifacts could be critical when doing metrology on outer structures. A good compromise between measurement time and reachable deviation is gained for the specimen tp07, when using a copper prefilter with a thickness between 0.5 mm and 1.0 mm.

4 Conclusions

We have presented a performance optimized simulation tool for X-ray cone beam computed tomography designed to improve the measurement of real world parts. We revealed some guidelines for the determination of a reasonable specimen alignment and applicable parameters for X-ray CBCT to minimize artifacts and measurement deviations. The influence of different measurement parameters on metrology has been investigated for a selected test part, by performing CT measurements, CT simulations and CMM measurements. We showed a comparison of measured and simulated CT results.
Based on this investigation we suppose that beam hardening could be critical when doing metrology on outer structures. Beam hardening could be reduced best by using prefilter plates or applying a correction algorithm. Increasing the acceleration voltage reduces measurement deviations, but not as much as a proper prefilter.

Acknowledgments

This work was supported by the “SimCT” project of the Austrian Research Promotion Agency grant number 812136-SCK/KUG and the “K-Project for non-destructive testing and tomography” grant number 820492.

References

[1] B.Chyba , M.Mantler, M.Reiter, ”Monte-Carlo simulations for evaluation of different influences on projections in computed tomography”, Denver X-Ray Conference 2009, Denver, United States of America, 2009.
[2] Carl Zeiss. Calypso - Visual metrology. Carl Zeiss – Industrielle Messtechnik: WWW: http://www.zeiss.de/calypso, 22th December 2009.
[3] D.Imkamp, J.Wanner, “Es geht auch einfach: Genauigkeitsangaben und Leistungstest für Koordinatenmessgeräte“, published by Carl Zeiss IMT GmbH, July 2005
[4] L.A.Feldkamp, L.C.Davis, and J.W.Kress, “Practical cone-beam algorithm“, J.Opt.Soc.Am. A / Vol. 1, No. 6/ June 1984.
[5] H.Ebel., XRS, 1999, 28,4, 255-266, and H.Ebel , „Advances in X-ray Analysis“, 2006, 49, 267-273.
[6] A.Koenig, A.Glière, „Radiographs simulation using system MTF“, Review of Progress in Quantitative Nondestructive Evaluation, vol. 19A, pp. 643-650, 2000.

[7] A.Brunetti, M. Sanchez del Rio, B. Golosio, A. Simionovici, A. Somogyi, Spectrochim Acta, 2004, B 59, 1725–1731.
[8] T.Möller, B.Trumbore., „Fast, Minimum Storage Ray-Triangle Intersection“, Journal of Graphics Tools, vol. 2, 21-28, 1997
[9] M.Reiter, M.M.Malik, C.Heinzl, D.Salaberger, E.Gröller, H.Lettenbauer, J.Kastner, Improvement of X-ray image acquisition using a GPU based 3DCT simulation tool, SPIE Quality Control by Artificial Vision Wels, AUSTRIA, May 27-29, 2009.
[10] B.D.Smith, “Image reconstruction from cone-beam projections: necessary and sufficient conditions and reconstruction methods”, IEEE Trans on Med. Image, Vol.MI-4, No.1, March 1985.